

# Advances in the Multiphysics Analysis of Structures <sup>(1)</sup>

by

Klaus-Jürgen Bathe

Massachusetts Institute of Technology  
Cambridge, MA 02139, USA

## Abstract

In this presentation we survey the advances that we have recently accomplished for the effective analysis of solids and structures, specifically for wave propagations and transient solutions, the analysis of shells, improved stress calculations, the use of interpolation covers, and the solution of the full Maxwell's equations. The structures may be subjected to complex fluid flows and electromagnetic effects. We briefly give the theoretical developments for the formulations, a few illustrative solutions, and conclude by mentioning some further exciting research challenges.

**Keywords:** Finite elements, multiphysics, wave propagations, shells, large strains, improvements of stresses, Maxwell's equations, electromechanics, fluid flows

## 1. Introduction

The analysis of solids and structures in multiphysics conditions has been given increasing attention during the recent years [1]. A large number of problems considered only a decade ago as very difficult to solve can now be analyzed with relatively little computational effort. However, there are many problem areas where significant advances are still needed for effective simulations. The objective in this paper is to briefly present some advances that we have recently accomplished. Due to space limitations, we mention only our books and papers and refer the reader to the many additional references given therein.

When considering research achievements in the field, it is important to realize the philosophy that a research group adheres to in its research on computational methods. *Our philosophy – as pursued for about 40 years now – is to focus on the development of methods that are general, reliable and efficient, and advance the current state of the art as practiced in industry and the sciences [1, 2].* We have not

---

<sup>(1)</sup>The paper is copyright Civil-Comp Ltd and will be presented at the Conference CST 2012, Dubrovnik, Croatia, Sept. 4 -7, 2012

pursued research that is claimed to open up new avenues when it is clear that such research will not lead to an advancement of the current state of the art. New avenues are only of interest if we see the potential for such an advancement. In all cases, our final aim – but of course not always reached – is that the methods we propose will ultimately be of use for a large community of engineers and scientists.

Indeed, the ultimate test as to whether a proposed computational scheme is of value is clearly given by whether it is used, once published, widely in industry and scientific investigations. This extensive use is driven forward by the keen interest in engineering and the sciences to solve ever more complex and difficult physical problems through finite element simulations.

Included in our research are the conception of novel methods, their mathematical analysis and their testing to establish the generality, reliability and efficiency.

A finite element method is *general* if it is applicable to many varied problems in a certain category of problems; for example, a general shell element can be used for all shell problems described by a general mathematical model like the ‘basic shell model’ identified in references [3, 4].

A finite element method is *reliable* and *efficient* if identified as such; for example, a finite element discretization is reliable and efficient if the ellipticity and inf-sup conditions are satisfied without the use of any artificial factors, and the scheme shows optimal convergence at a low computational cost [1, 2, 4, 5].

To show whether a method is reliable and efficient requires mathematical analysis as far as such is possible and well-designed numerical tests [1, 2, 4]. Both, the mathematical analyses and the benchmark tests, can frequently not ‘prove’ that a method is always efficient – considering for example general nonlinear analysis – but these efforts can give significant insight into numerical schemes.

The objective in this presentation is to briefly summarize our research efforts to advance the state of computational simulations with the above research aims in mind. In the next sections, we present our recent developments regarding the analysis of wave propagation problems, the analysis of shells, the prediction of more accurate stresses, the use of interpolation covers to increase the convergence of finite element discretizations, and the simulation of electromagnetic effects and their coupling to structures and fluid flows. Since each of these developments covers a large field, we can give in this paper only a brief summary of our developments and need to refer the reader to our papers written on these topics.

## **2. Some Recent Developments**

In the following sections, we focus briefly on the basic ideas and some results and refer to our papers for details on the research. When we give here solid mechanics solutions, the procedures are also applicable in multiphysics analyses.

## 2.1 The solution of wave propagation problems

Although much research effort has been expended on the solution of wave propagation problems using finite element methods, the accurate simulation of transient wave propagations and the accurate solution of harmonic problems at high frequencies have remained a significant challenge. Such problems are abundantly encountered, for example, in solid and structural mechanics, seismic engineering, and in electromagnetics. The essential difficulty is that to capture the high frequency response seen in wave propagations, extremely fine meshes of conventional finite elements are needed. However, even with such very fine meshes in transient solutions, spurious oscillations are calculated near the wave fronts, and numerical dispersion and dissipation of waves due to the spatial and temporal discretizations are observed. Hence, spectral methods, spectral element methods, and spectral finite element methods have been proposed but these are not as general and effective as needed in engineering practice.

We have developed a finite element method ‘enriched for wave propagation analyses’ [6]. This method shows considerable promise in that the standard low-order Lagrangian finite element interpolations are simply enriched with harmonic functions, governed, as usual, by nodal degrees of freedom. An important point is that the usual fundamental theory of finite element methods is applicable.

For two-dimensional solutions, the basic displacement interpolations for a typical solution variable  $u(r,s)$  are

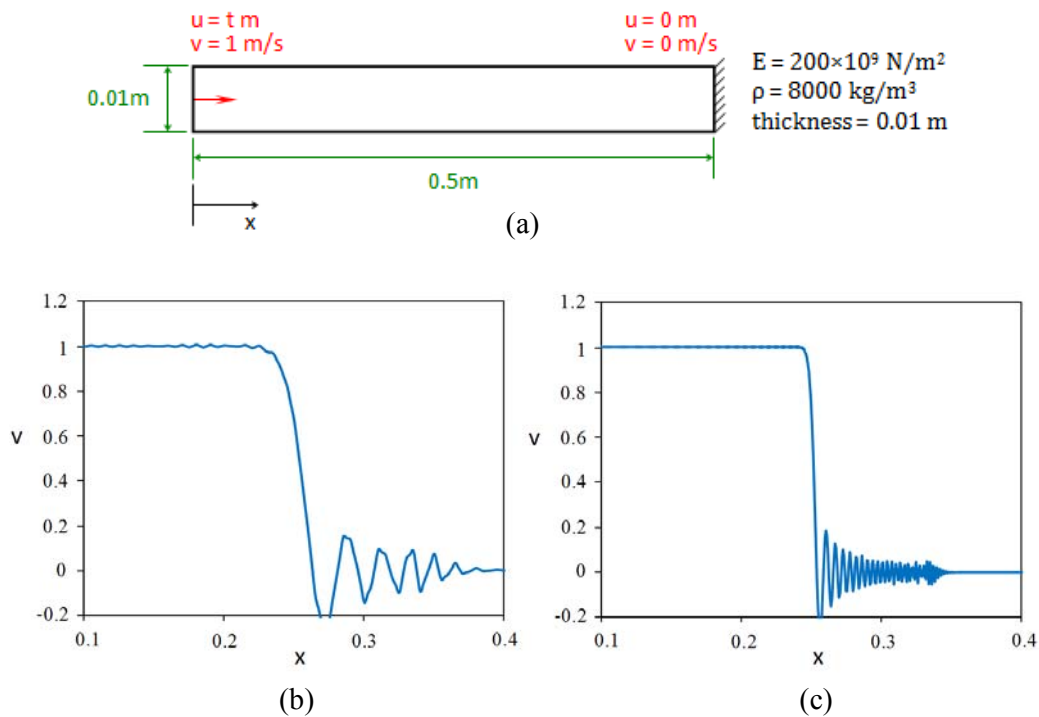
$$\begin{aligned}
 u(r,s) = & \\
 & \sum_{\alpha} h_{\alpha}(r,s) \\
 & \left[ \begin{aligned}
 & U_{(\alpha,0,0)} + \sum_{k_x=1}^n \left\{ \cos\left(\frac{2\pi k_x x}{\Lambda_x}\right) U_{(\alpha,k_x,0)}^c + \sin\left(\frac{2\pi k_x x}{\Lambda_x}\right) U_{(\alpha,k_x,0)}^s \right\} \\
 & + \sum_{k_y=1}^m \left\{ \cos\left(\frac{2\pi k_y y}{\Lambda_y}\right) U_{(\alpha,0,k_y)}^c + \sin\left(\frac{2\pi k_y y}{\Lambda_y}\right) U_{(\alpha,0,k_y)}^s \right\} \\
 & + \sum_{k_x=1}^n \sum_{k_y=1}^m \left\{ \begin{aligned}
 & \cos\left(\frac{2\pi k_x x}{\Lambda_x} + \frac{2\pi k_y y}{\Lambda_y}\right) U_{(\alpha,k_x,k_y)}^{c+} + \sin\left(\frac{2\pi k_x x}{\Lambda_x} + \frac{2\pi k_y y}{\Lambda_y}\right) U_{(\alpha,k_x,k_y)}^{s+} \\
 & + \cos\left(\frac{2\pi k_x x}{\Lambda_x} - \frac{2\pi k_y y}{\Lambda_y}\right) U_{(\alpha,k_x,k_y)}^{c-} + \sin\left(\frac{2\pi k_x x}{\Lambda_x} - \frac{2\pi k_y y}{\Lambda_y}\right) U_{(\alpha,k_x,k_y)}^{s-}
 \end{aligned} \right\}
 \end{aligned} \right] \quad (1)
 \end{aligned}$$

where the  $U_{(\alpha, k_x, k_y)}$  with superscripts are the nodal degrees of freedom,  $\alpha$  is the local element node, with  $h_\alpha$  the conventional finite element interpolation function, and the  $S$ ,  $C$ , and  $+$  and  $-$  are used in the superscripts to correspond to the harmonic expressions. These interpolation functions can be written using exponentials on the complex plane, but in the analysis of solids using only real arithmetic can be much more effective. Of course, the interpolations for one- and three-dimensional analyses directly follow from equation (1). Here, the two fundamental wavelengths  $\Lambda_x$  and  $\Lambda_y$ , and the wave cut-off numbers  $n$  and  $m$  with  $1 \leq k_x \leq n$ ,  $1 \leq k_y \leq m$ , and typically  $n, m \leq 3$ , need to be chosen by the analyst as part of the model data.

As example solutions, we consider the field of transient analyses and the field of harmonic problems, each with an illustrative solution.

### 2.1.1 A transient solution: 1D impact of an elastic bar

This special 1D problem, shown in Figure 2.1-1, can be solved accurately using explicit time integration with 2-node linear elements and a lumped mass matrix [2], and also using the Bathe implicit time integration [7, 8] (with a consistent mass matrix and CFL number = 1.0). However, just to test the enriched finite element formulation, we solved the problem using uniform meshes of 2-node linear elements, consistent mass matrices, and the trapezoidal rule with the very small time step  $\Delta t = 2.5 \times 10^{-8} s$  (resulting into significant oscillations in the response).



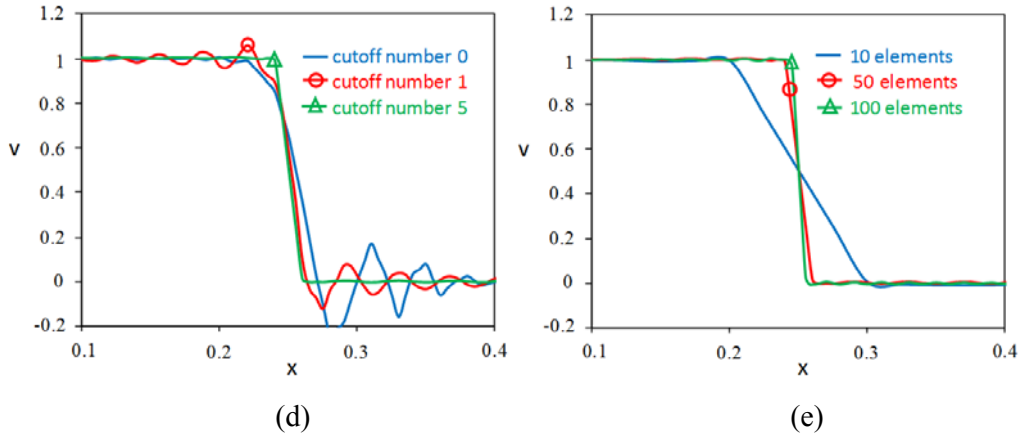


Figure 2.1-1. Solution of impact of a bar, at time 0.00005s; (a) elastic bar considered; (b) with 100 traditional linear elements; (c) with 700 traditional linear elements; (d) with 50 linear enriched elements; (e) with cutoff number 5

Figure 2.1-1 shows the well-known spurious oscillations in the velocity and hence stress predictions. In this case, using the enriched finite elements we can control the large spurious high-frequency oscillations and make them acceptably small. But more studies are needed to identify in how far this solution behavior is applicable in 2D and 3D analyses and how effective the procedure is in practice.

### 2.1.2 A time harmonic solution: 2D acoustic pressure wave

Here we consider the solution of the Helmholtz problem (see Figure 2.1-2)

$$\begin{aligned}
 \nabla^2 P + k^2 P &= 0 && \text{in } V, \\
 \frac{\partial P}{\partial n} &= g(x, y) && \text{on } S_f, \\
 \lim_{r \rightarrow \infty} \sqrt{r} \left( \frac{\partial P}{\partial r} - ikP \right) &= 0.
 \end{aligned} \tag{2}$$

where  $P(x, y)$  is the unknown harmonic pressure,  $k = \omega/c$ ,  $r$  is the distance from the origin in the Cartesian coordinates, and  $n$  is the unit normal on  $S_f$ .

For the numerical test solution, we prescribed  $g(x, y)$  given by the analytical solution and used  $k = 22.06$ . Figure 2.1-2 shows the analytical solution and the mesh for our finite element solution. We should note the rather coarse mesh used.

Included in the mesh is a ‘perfectly matched layer’ to model the infinity of the physical domain.

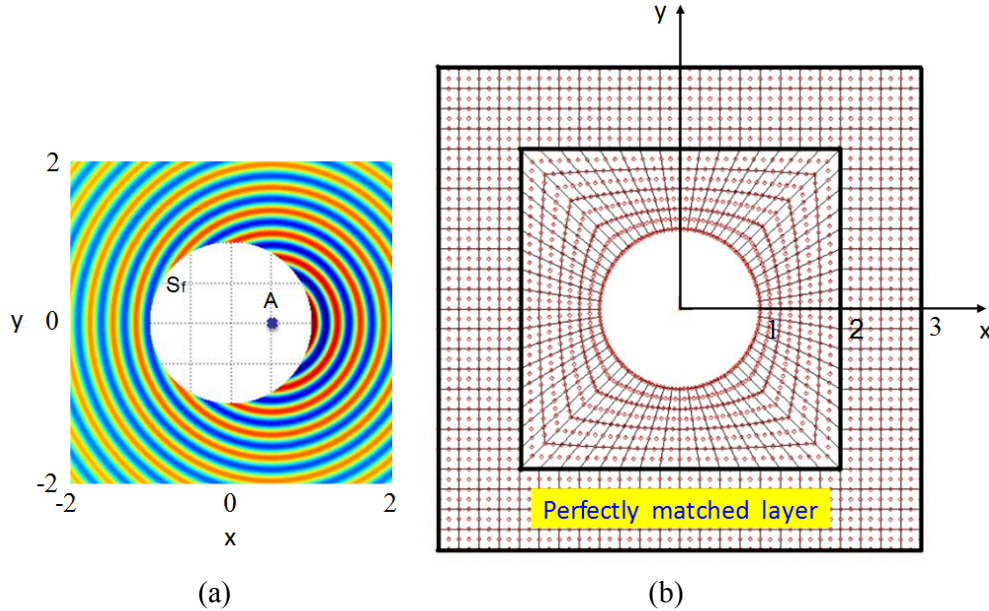


Figure 2.1-2. Solution of pressure wave; (a) the analytical pressure, A is the pole at  $(x_0, y_0) = (0.5, 0)$ ; (b) mesh of 9-node elements

Figure 2.1-3 gives contour plots of the pressure numerical solutions using the cutoff numbers from 0 to 2 and the convergence in the  $L^2$  norm (although a better norm might be used). We note that the result obtained using the cutoff numbers  $(n, m) = (2, 2)$  is in good agreement with the analytical solution.

While, as earlier mentioned, we employ mostly only real arithmetic, actually, in this example solution we used complex arithmetic for the perfectly matched layer in the discretized domain.

## 2.2 The analysis of shells

Significant research efforts over some decades have been spent on the analysis of shells, but there are still many outstanding challenges in the field of shell analysis [4]. In the following, we focus on two important items, namely the proper benchmark testing of shell elements and the analysis of large strain conditions in shells.

### 2.2.1 The testing of shell elements

Commonly, shell elements have been tested in linear analysis by solving plate and some well-known shell problems, like the pinched cylinder, Scordelis-Lo, and

hemispherical shell problems, but not including a shell of negative Gaussian curvature. In these solutions, some displacements at certain points are measured. It should, however, be recognized that such solutions do not constitute a thorough assessment of the capabilities of a shell solution scheme. Instead, it is important to measure the scheme on the following criteria:

- As basic requirements, the shell element used should not be based on artificial factors, not contain any spurious modes and be geometrically isotropic.

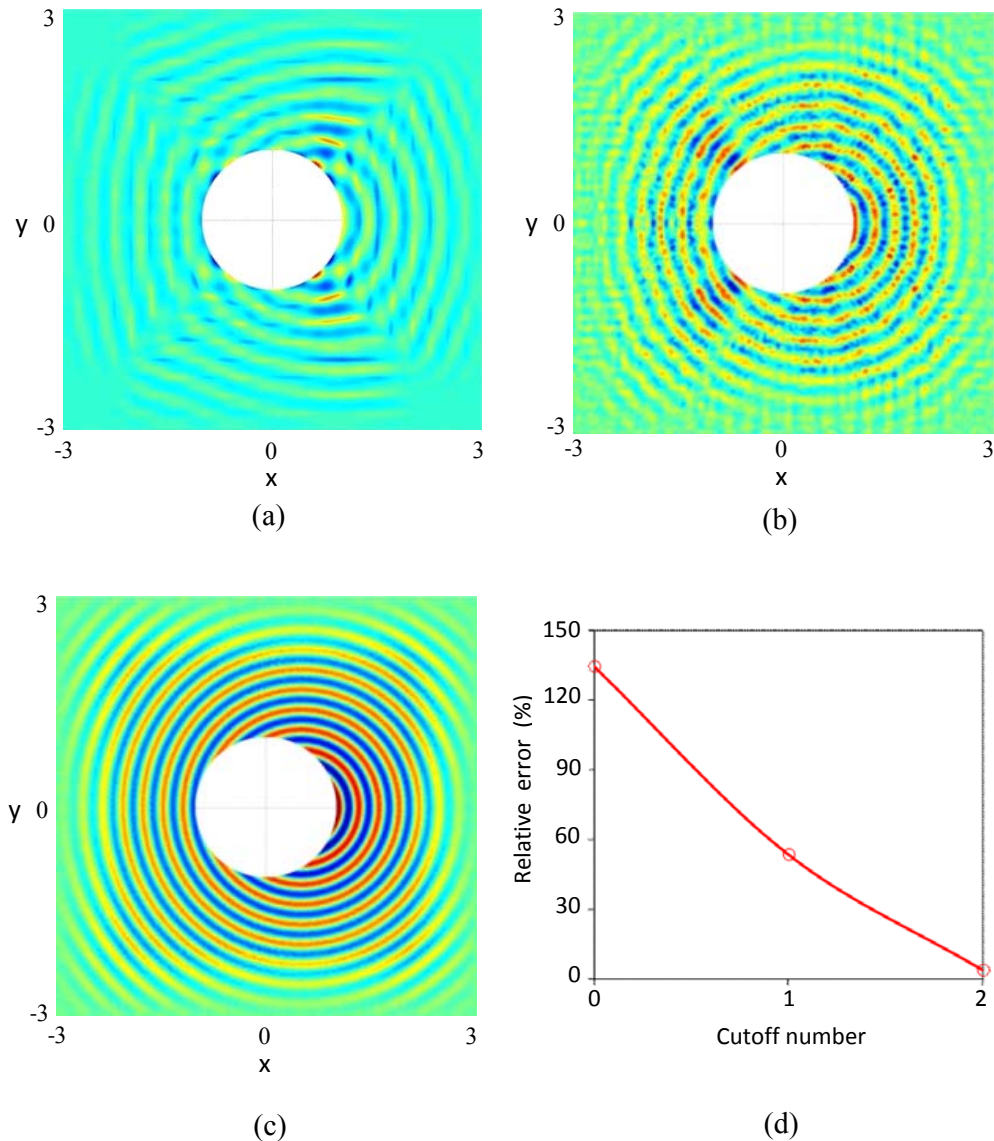


Figure 2.1-3. Numerical solutions: (a)  $(n,m)=(0,0)$ , (b)  $(n,m)=(1,1)$ , (c)  $(n,m)=(2,2)$  and (d) relative error in  $L^2$  norm not including the perfectly matched layer

– The element should be tested in the solution of the hyperboloid shell problems shown in Figure 2.2-1, or similar problems of shells with negative Gaussian curvature, and in these solutions proper norms should be used.

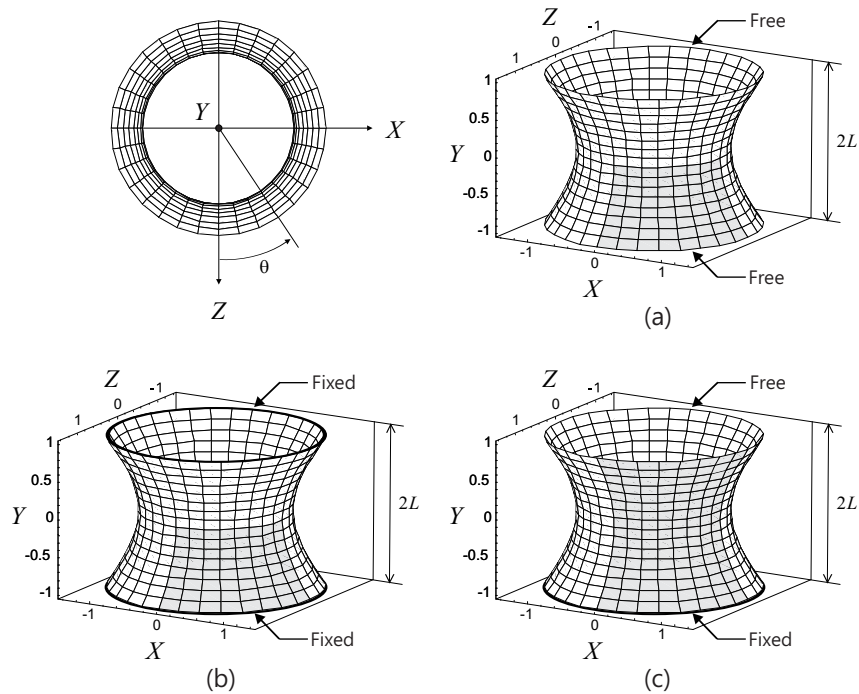


Figure 2.2-1. Three shell test problems;  $L = 1.0$ ,  $E = 1.0 \times 10^{11}$ ,  $\nu = 1/3$

The shell surfaces in Figure 2.2-1 are given by  $X^2 + Z^2 = 1 + Y^2$  and the loading is the pressure  $p(\theta) = \cos(2\theta)$ . Only the shaded regions in the figure are modeled.

As discussed in references [4, 9], the use of an appropriate norm in the error measure is very important. Using the s-norm defined in these references, we present the test results obtained using the MITC4 shell element in Figure 2.2-2. This element satisfies of course the basic requirements mentioned above and, as seen in Figure 2.2-2, performs very well in the analysis of the shell problems. For details on the testing of plate and shell elements we refer to references [4, 9-11].

### 2.2.2 The large strain analysis of shells

The large strain analysis of shells is pursued in many applications of science and engineering. Examples occur in biomechanical situations and in the crush and crash analyses of structures.



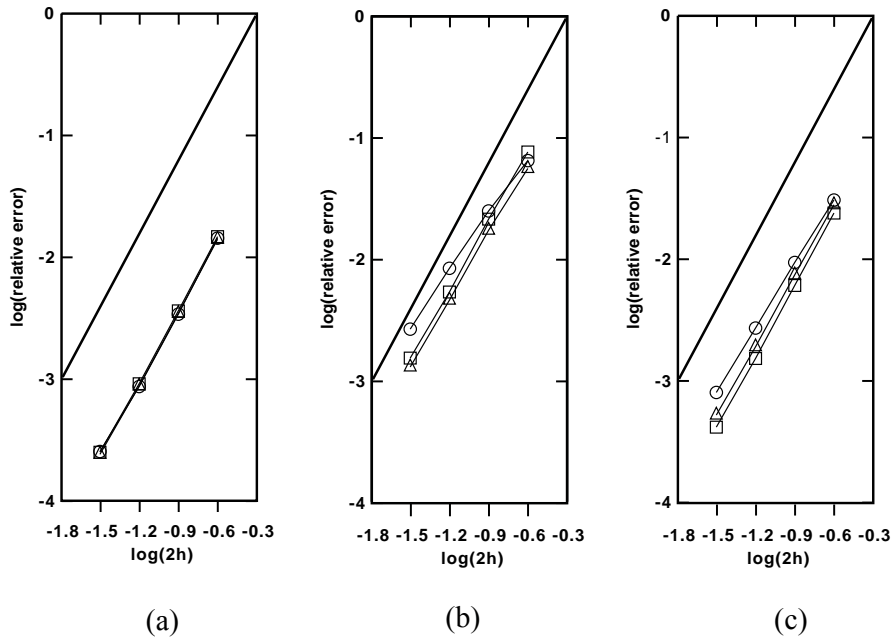


Figure 2.2-2. Convergence curves for the MITC4 shell element used in the three problems of Figure 2.2-1, for decreasing shell thickness, using the s-norm; (a) free-free shell; (b) fixed-fixed shell; (c) fixed-free shell; see reference [9]

We have developed 3-node and 4-node 3D-shell elements that build upon the classical MITC shell elements but that include important three-dimensional effects [12]. The elements can be used to model very large deformations with large plastic strains using the Updated Lagrangian Hencky total strain formulation [2, 13]. An important point is that the 3D-shell elements can be employed in explicit and implicit dynamic solutions and in static analyses, since no reduced integration with hourglass control is used and there are no artificial stabilization factors in the formulation. The 3D-shell elements can be employed like the conventional MITC shell elements with 5 or 6 degrees of freedom at each node, but, when invoked by additional nodal degrees of freedom at the shell mid-surface, the elements represent through-the-thickness straining (2 extra degrees of freedom) and warping of the transverse fibers (2 or 3 extra degrees of freedom). Thus, while all degrees of freedom are defined at the shell mid-surface nodes in accordance with a shell theory, from a displacement interpolation point of view, the elements can be thought of as higher-order 3D solid elements, with assumptions, when the additional degrees of freedom are invoked.

In the formulations, MITC interpolations are used to prevent shear locking, and in incompressible analysis the u/p formulation is employed [2, 14]. A particular aspect addressed in reference [12] is to give benchmark solutions for large strain analyses.

Figure 2.2-3 shows an application in a large strain solution that represents a good benchmark test [12]. Here the large strains in the structure result into a significant downward shifting of the mid-surface nodes during the response.

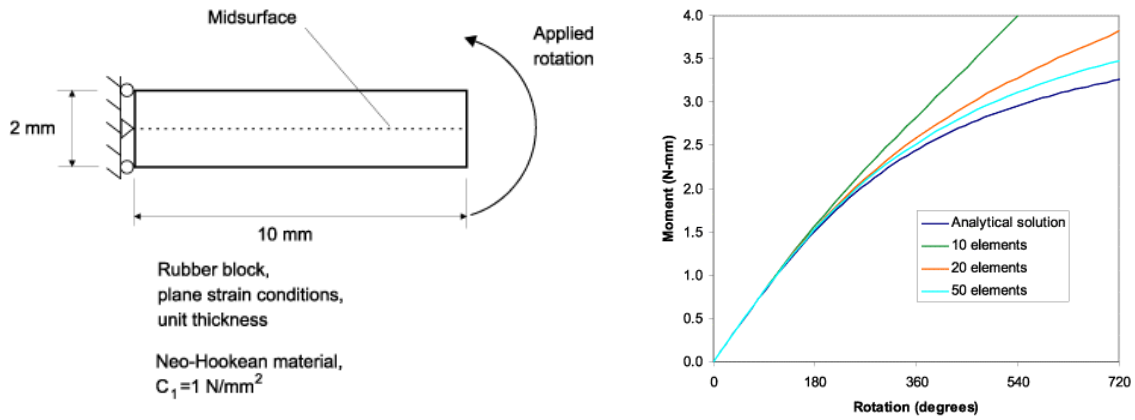
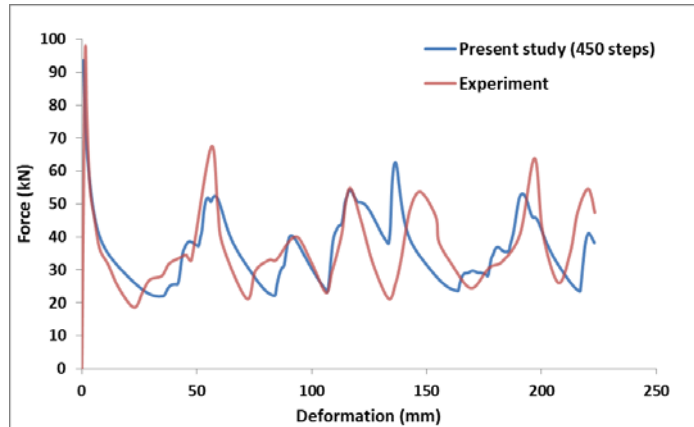


Figure 2.2-3. Large strain analysis of thick cantilever; incompressible Mooney-Rivlin material; the MITC4 3D-shell element is used

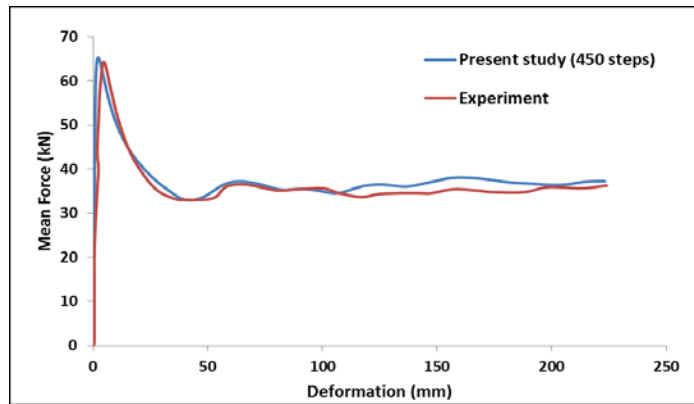
Figure 2.2-4 shows some analysis results using the MITC4 3D-shell element in a slow crush analysis and Figure 2.2-5 shows crash solution results, all obtained using the Bathe implicit time integration scheme, for details see reference [15].



(a)



(b)



(c)

Figure 2.2-4. Quasi-static crushing of a square-section tube, length of tube is 310 mm; (a) experimental and computed results in final configuration; (b) force - displacement curves; (c) mean crushing force - displacement curves

Here, the important point is that the same elements are employed to solve static and dynamic problems. Of course, since full numerical integration is used, solutions with explicit time integration are computationally quite expensive compared to when using elements based on reduced integration and hourglass control.

### 2.3 A procedure for stress improvements

It is well known that the low-order displacement-based finite elements (3-node triangular and 4-node quadrilateral elements in 2D solutions, and 4-node tetrahedral and 8-node brick elements in 3D solutions) are not effective in predicting stresses accurately. Very fine meshes are needed in practice. On the other hand, the elements

are quite robust, and the bandwidth of the resulting finite element equations is relatively small. Hence, if the order of stress convergence could be increased, the elements would be quite attractive in various analyses.

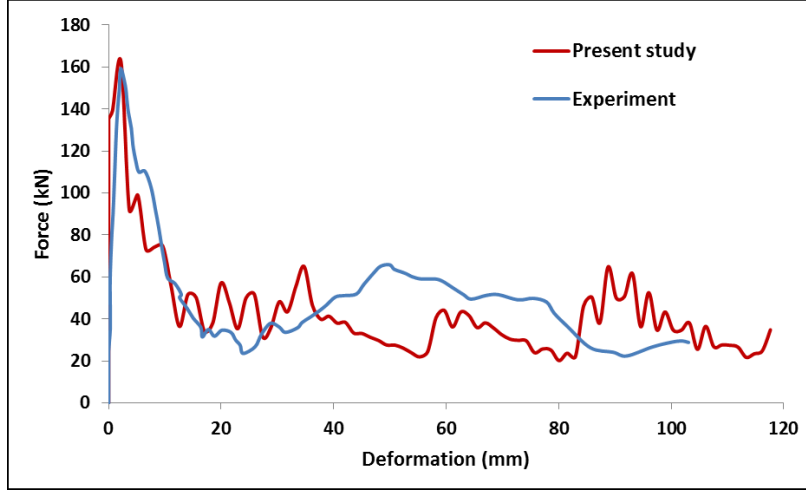


Figure 2.2-5. Force-displacement curves in fast crashing of a square section tube, tip velocity is 54 km/hr, initial length of tube is 310 mm

We have developed a novel and promising ‘stress improvement scheme’ for these elements. The procedure is simple and inexpensive to use, and we have found that in 1D and 2D solutions, based on some analysis but mostly numerical experiments, the stresses converge at a quadratic rate, or close thereto, which is optimal since the displacements converge at that rate. The derivation of the basic equations used is given in reference [16]. These equations are the usual virtual work statement for the displacement-based finite element solution

$$\sum_{m=1}^N \left( \int_{V^{(m)}} \delta \underline{\varepsilon}^{(m)T} \underline{C}^{(m)} \underline{\varepsilon}^{(m)} dV - \int_{S_f^{(m)}} \delta \underline{u}^{(m)T} \underline{f}^S dS - \int_{V^{(m)}} \delta \underline{u}^{(m)T} \underline{f}^B dV \right) = 0 \quad (3)$$

and the two projection equations

$$\sum_{m=1}^{N_p} \left( \int_{V^{(m)}} \delta \underline{\tau}^{(m)T} \left\{ \underline{\tau}^{(m)} - \underline{\tau}_h^{(m)} \right\} dV \right) = 0 \quad \forall \quad \underline{\tau}^{(m)} \in \bar{V}^\tau \quad (4)$$

$$\sum_{m=1}^{N_p} \left( \int_{V^{(m)}} \delta \underline{\zeta}^{(m)T} \left\{ \text{div} \left[ \underline{\tau}^{(m)} \right] + \underline{f}^B \right\} dV \right) = 0 \quad \forall \quad \underline{\zeta}^{(m)} \in P_1 \quad (5)$$

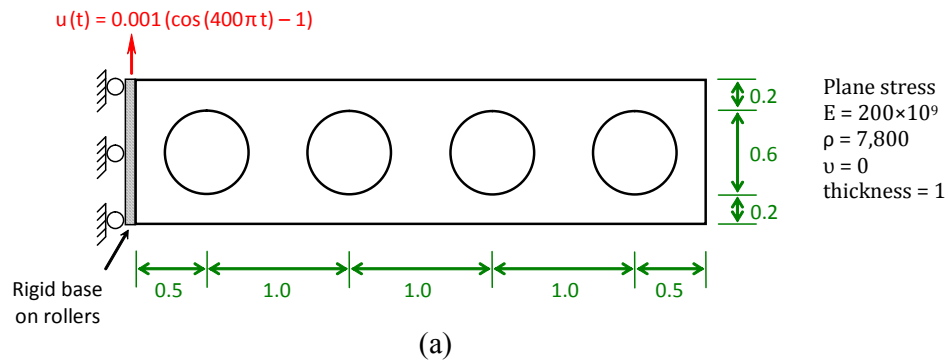
where  $P_k$  denotes the  $k$ th order polynomial,  $\underline{\tau}^{(m)}$  represents the enhanced stresses to be calculated in  $P_2$ ,  $\underline{\tau}_h^{(m)}$  the directly-calculated stresses, and  $\bar{\tau}^{(m)}$  an element in  $\bar{V}^r$ , the subspace of  $P_2$  in which all stress functions satisfy the equilibrium equations  $div[\bar{\tau}^{(m)}] = \underline{0}$ , and  $N_p$  is the number of elements in the stress domain considered. For the additional notation we refer to references [2, 16].

The first projection equation, Equation (4), expresses in essence that, integrated over the stress calculation domain, the enhanced stresses projected onto the space of the self-equilibrating stresses shall be equal to the directly-calculated stresses projected onto that space. Hence, this equation somewhat extracts from the directly-calculated stresses that part which is of good quality. The second projection equation, Equation (5), then sets to zero the difference in the divergence of the enhanced stresses and the exact stresses in the projection onto the space  $P_1$ . Assuming a quadratic variation in stresses, the scheme results into a set of algebraic equations in the unknown stress coefficients for which the coefficient matrix is well conditioned and the equations are inexpensive to solve.

This new stress enhancement procedure is compared with other previously published attractive schemes in reference [16]. The important attributes are that the new method is effective and can be used in linear static and dynamic analyses, and, since geometrically distorted elements present no difficulty, in nonlinear solutions.

Figure 2.3-1 shows the results obtained in the dynamic analysis of a cantilevered plate with holes. Since it is important to predict the accelerations accurately (which enter as body forces in Equation (5)), we use the Bathe time integration scheme, see references [8, 16]. The excellent convergence rate for the stresses is seen.

Figure 2.3-2 shows the results calculated in the static analysis of a large strain problem. Here too excellent results have been obtained. Finally, we should note that the scheme may be used to establish solution error measures, and while here applied to solid mechanics problems is clearly also applicable in multiphysics analyses.



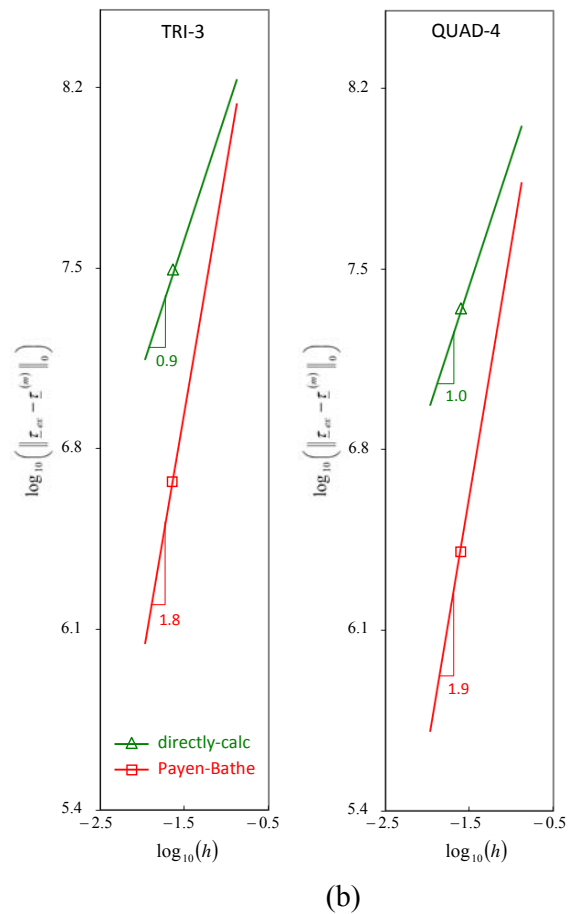
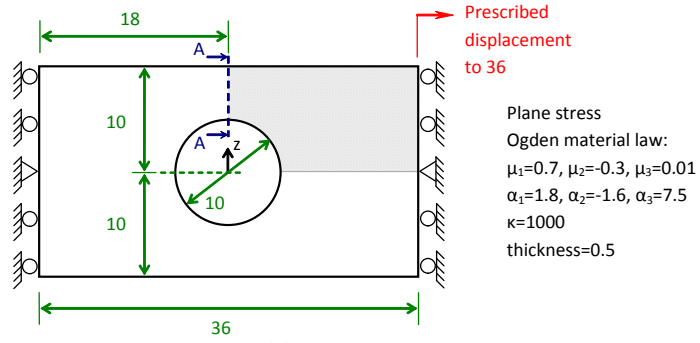


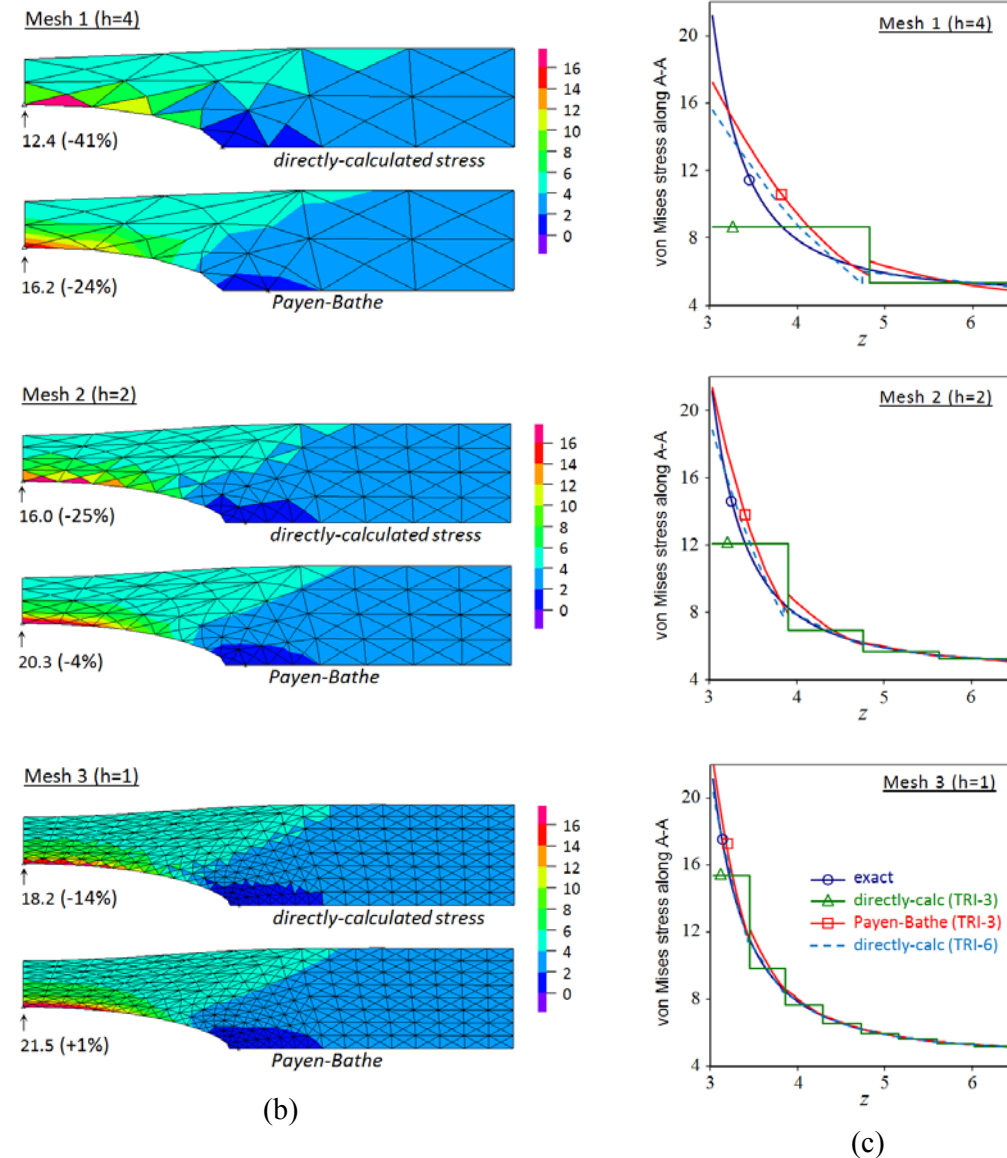
Figure 2.3-1. Dynamic analysis of cantilevered plate; the stresses are sought at time = 0.01902; (a) problem solved; (b) convergence rates

The computational expense to obtain improved stresses is given by the numerical effort involved in solving for 18 unknown stress coefficients in 2D solutions (and 60 unknown stress coefficients in 3D solutions), for each element  $m$  in the areas where stresses are to be improved. Of course, in practice, the stresses may only be improved in certain areas.

We have found this expense to be small in 2D solutions, as compared to establishing the global stiffness matrix and solving the equations of equilibrium of the total finite element assemblage. Indeed, in a typical linear static analysis with  $10^5$  degrees of freedom, the expense to calculate the improved stresses for all elements in the assemblage is probably about 1 % of the total solution cost. Considering 3D solutions, the expense is probably also low but actual testing should be performed.



(a)



(b)

(c)

Figure 2.3-2. Stress improvement in analysis of a large strain problem; (a) problem solved; (b) von Mises band plots; (c) von Mises stress along section A-A

## 2.4 The enrichment of finite element solutions using interpolation covers

The scheme given in section 2.3, of course, only improves, inexpensively, the stresses. For the low-order finite elements, we have also developed a scheme to improve all solution variables by ‘enriching the finite element discretization with interpolation covers’ [17]. These covers are applied over element patches in certain areas where higher accuracy in the solution variables is sought, like higher accuracy in the displacements and stresses. The procedure is closely related to previously published schemes, see reference [17].

Consider the patch of 2D 3-node elements shown in Figure 2.4-1. The essence of the enrichment scheme is to interpolate the degree of freedom at node  $i$  over the patch of elements, which gives for the element

$$u_h = \sum_{j=1}^3 h_j u_j + \sum_{j=1}^3 \tilde{h}_j \tilde{u}_j \quad \text{in the element}$$

where we sum over the nodes  $s_1, s_2, s_3$ , and, for node  $j$ ,  $u_j$  is the usual nodal degree of freedom and  $\tilde{u}_j$  lists the additional degrees of freedom with

$$\tilde{h}_j = h_j [\bar{x}_j \quad \bar{y}_j \quad \bar{x}_j^2 \quad \bar{x}_j \bar{y}_j \quad \bar{y}_j^2 \quad \cdots \quad \bar{y}_j^p]$$

Here the  $(\bar{x}_j, \bar{y}_j)$ -coordinates are measured from node  $j$ , see Figure 2.4-2.

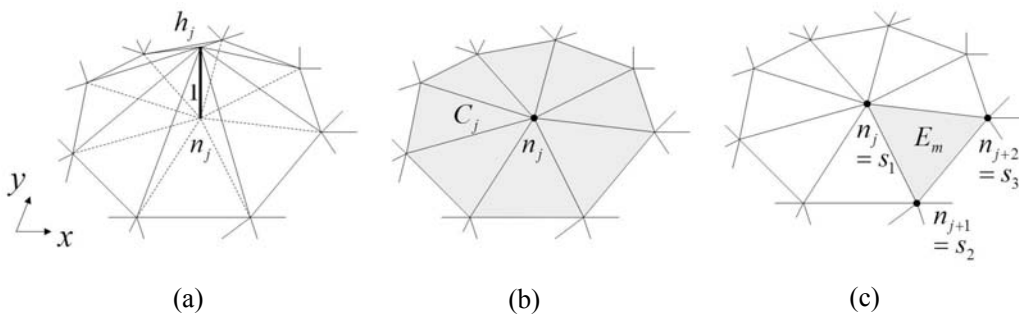


Figure 2.4-1. Description of interpolation cover; (a) usual nodal displacement function; (b) elements affected by the cover; (c) an element



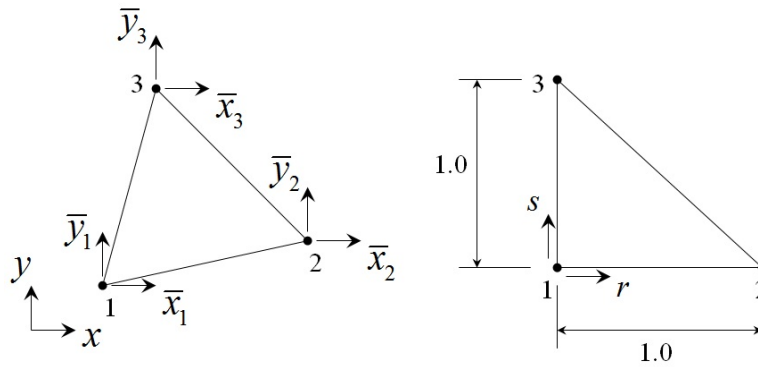


Figure 2.4-2. Coordinate systems for a triangular 3-node element

In the use of the method, we only apply the covers on interior mesh nodes and not on the boundaries where boundary conditions are applied as usual.

Figures 2.4-3 and 2.4-4 show some results obtained using this method [17]. While these solutions are for problems in solid mechanics, of course, the method is equally applicable in fluid flows, heat transfer and general multiphysics solutions.

However, since the nodal variables for the cover interpolations couple into the usual degrees of freedom, all of these must be solved for together. Hence the effectiveness of the scheme needs to still be evaluated for general 2D and 3D solutions where also higher-order elements might be used instead of the cover interpolations.

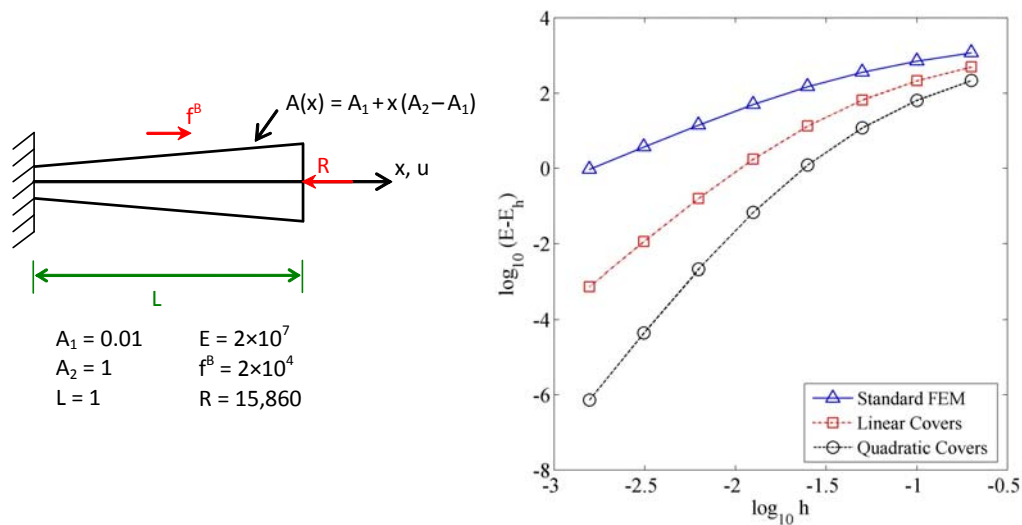


Figure 2.4-3. Analysis of 1D bar; uniform meshes are used

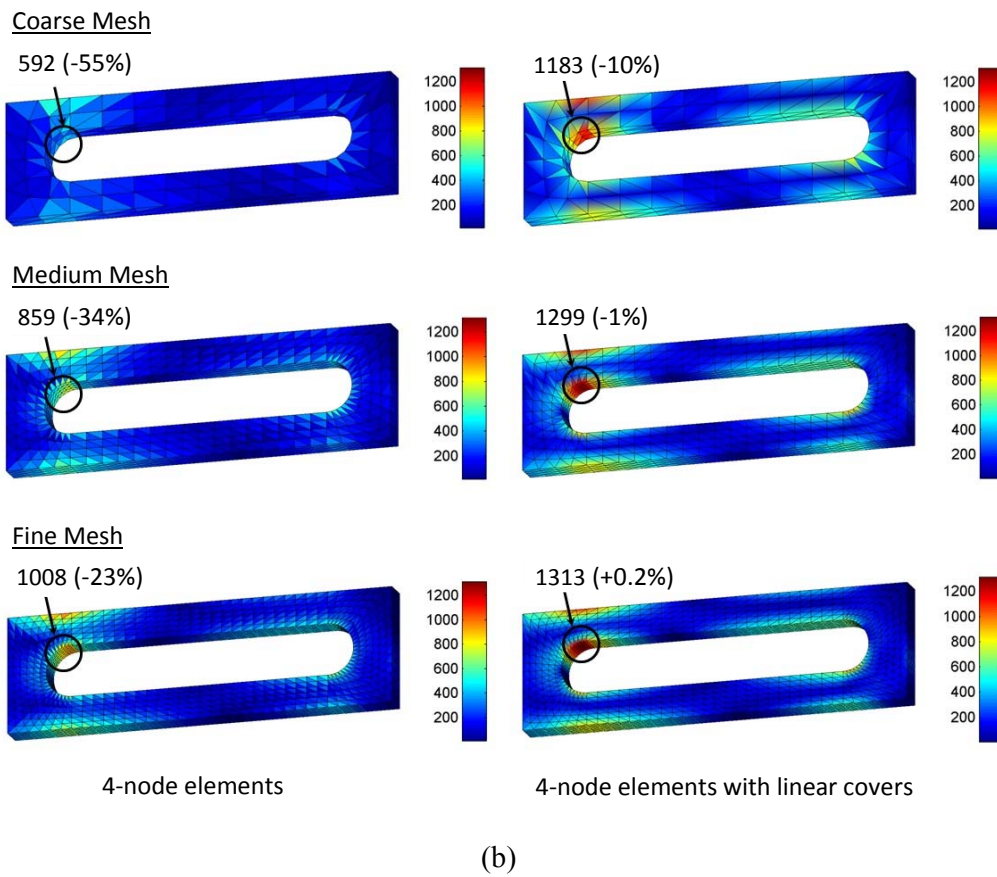
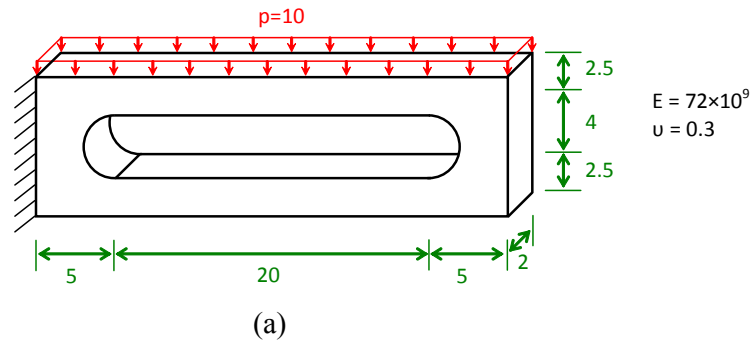


Figure 2.4-4. 3D analysis of machine tool jig; (a) problem solved; (b) the solutions on the left correspond to the use of the traditional 4-node tetrahedral finite elements, the solutions on the right were obtained using linear interpolation covers; the errors are given in parentheses

## 2.5 The coupling of structures to fluid flows and electromagnetic effects

While the separate solution of fluid-structure interactions and electromagnetic problems has been pursued for decades, the solution of problems in which general structures interact fully coupled with fluid flows and electromagnetic effects has hardly been tackled and presents special difficulties. The coupled effects can be particularly important, for example, in problems of biomedical engineering, metal processing, and plasma physics, see reference [18].

A large number of publications are available on the numerical solution of electromagnetic field problems. In the most general cases, the full Maxwell's equations are solved. Considering the earlier proposed schemes, frequently spurious modes have been calculated and hence the solution schemes were not reliable. Thereafter, novel formulations were established, and in particular, edge-based elements. These elements are more reliable but have various shortcomings, including specifically that they do not couple directly with structural and fluid flow discretizations.

We developed in our research a novel finite element scheme for the solution of the general Maxwell's equations specifically to calculate electromagnetic effects coupled with fluid flows, solids and structures. In our solution procedure, we use either the primitive variables of electric and magnetic fields ( $\mathbf{E}$  and  $\mathbf{H}$ ) or the scalar electric and vector magnetic potentials ( $\phi$  and  $\mathbf{A}$ ) for static and harmonic solutions of problems governed by the full Maxwell's equations, including high frequency conditions. The finite elements used are similar to those we proposed for the solution of the Navier-Stokes equations, and the full coupling between the different physical phenomena is achieved as in fluid-structure interaction analyses [19, 20].

The basic equations we solve are, considering Faraday's law and Ampere's law with the Maxwell term, in the  $\mathbf{E}$ - $\mathbf{H}$  form

$$\nabla \cdot \left( (p + \rho_0 / \varepsilon^*) \mathbf{I} - \nabla \mathbf{E} + \mathbf{I} \times \mathbf{K} \right) = \mathbf{0} \quad \text{in } \Omega_e$$

and

$$\nabla \cdot (q \mathbf{I} - \nabla \mathbf{H} - \mathbf{I} \times \mathbf{J}) = \mathbf{0} \quad \text{in } \Omega_m$$

where  $\Omega_e$  and  $\Omega_m$  denote the domains of electric and magnetic fields, respectively,  $\mathbf{K}$ ,  $\mathbf{J}$  and  $\rho_0$  are the electric field, current and charge source terms,  $\varepsilon^*$  is the effective permittivity (for static and harmonic solutions),  $\mathbf{I}$  is the identity tensor, and we introduced

$$\begin{aligned} p &= \nabla \cdot \mathbf{E} - \rho_0 / \varepsilon^* \\ q &= \nabla \cdot \mathbf{H} \end{aligned}$$

Of course, these equations specialize to specific cases, by omitting certain terms, and the equations must be used with appropriate boundary and interface conditions.

However, for certain problems, a potential formulation can be more effective, in which the electric and magnetic potentials are used

$$\mathbf{E} = -\nabla\phi - \frac{\partial\mathbf{A}}{\partial t}; \quad \mathbf{B} = \nabla \times \mathbf{A}$$

with  $\nabla \cdot \mathbf{A} = g_A$  and  $g_A$  a gauge condition.

The electromagnetic effects couple into the fluid flows and structures due to Lorentz forces and due to Joule heating. The Lorentz body forces are

$$\mathbf{f}_b^{em} = \nabla \cdot \mathbf{T}^{em} + \mathbf{T}_b^{em}$$

with the Maxwell components  $\mathbf{T}^{em}$  and  $\mathbf{T}_b^{em}$  including electric and magnetic effects.

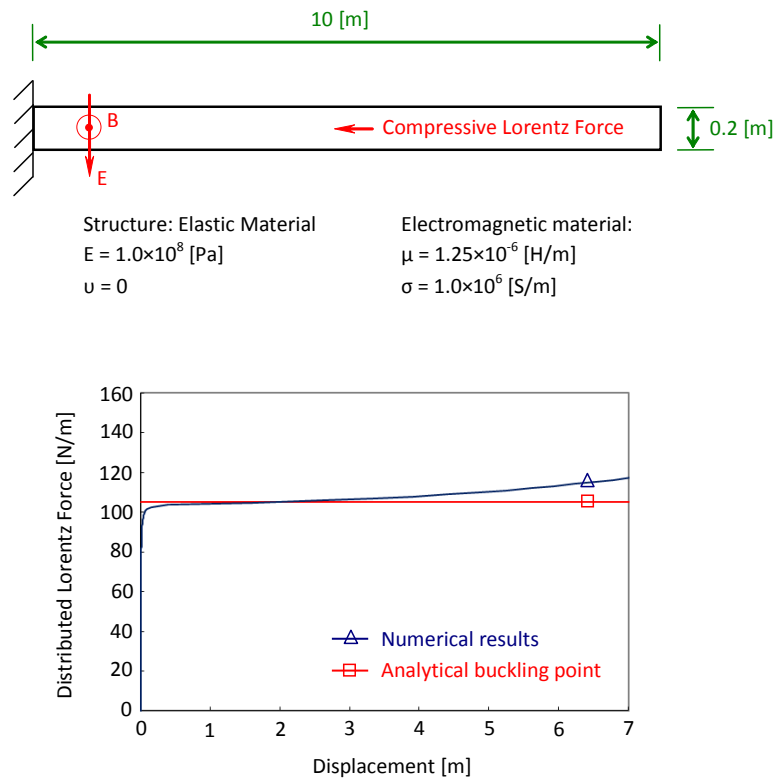


Figure 2.5-1. Buckling of beam due to Lorentz forces

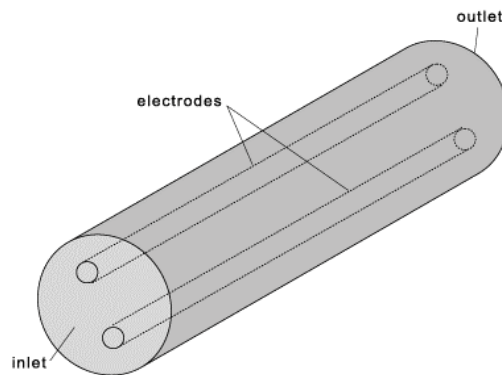
The heat generated by electromagnetic variables is calculated according to Joule's law as

$$q_b^{em} = \sigma^{-1} \mathbf{J} \cdot \mathbf{J}$$

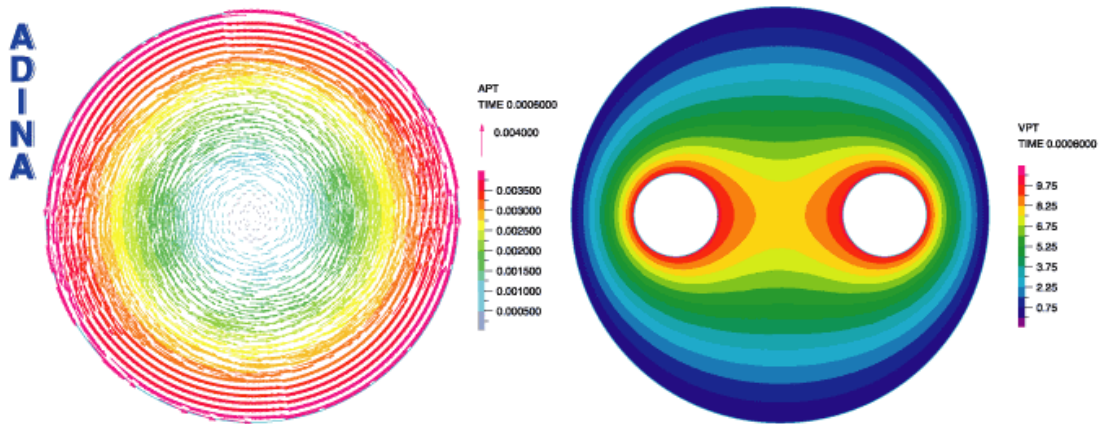
in which  $\sigma$  is the conductivity and  $\mathbf{J}$  is the current solved for. For details on the finite element formulations, see reference [18].

To consider a simple example, for comparison with an analytical solution, Figure 2.5-1 shows results for a beam that buckles due to electromagnetic force effects. Here the magnetic field intensity  $\mathbf{H}$  is almost constant while the electric field intensity  $\mathbf{E}$  is increased to obtain the increasing Lorentz force.

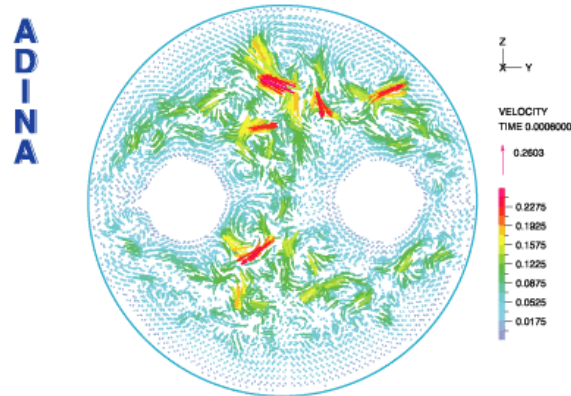
The solution of an additional problem is given in Figure 2.5-2, which shows the results of the mixing in a fluid flow driven by electromagnetic forces. Here the generated current and the magnetic field result into Lorentz forces that cause chaotic mixing in the fluid.



(a)



(b)



(c)

Figure 2.5-2. Electromagnetic chaotic mixing in channel; (a) the channel with the electrodes; (b)  $\mathbf{A}$  and  $\phi$  potentials; (c) velocity vector plot near inlet

### 3. Concluding Remarks

In this paper we presented some of the research we have pursued during the recent years. We focused on reliable and effective procedures to advance the multiphysics analysis of solids and structures.

There are many exciting research and development tasks still to be tackled in the field of computational simulations – in particular when the actual *practice* of simulations in engineering and the sciences is focused upon. Here the reliability of procedures is very important.

Considering the research presented in this paper, the *enrichment procedure for wave propagation analyses* shows much promise, but needs further studies focusing on its effectiveness, its use in shell analyses, and its use in explicit time integration. More *research on shell analyses* in general is needed but also specifically to obtain more effective triangular shell elements. The *procedure for stress improvements* could be applied to shell analyses as well, and the *method of cover interpolations* should be researched for nonlinear analysis and shell solutions. The analysis of *electromagnetic effects coupled to solids and fluids* is a very large field with many exciting research tasks that should include nonlinear effects and wave propagations.

In addition to the research areas mentioned above, we are working on the development of faster solvers, simulations in biological engineering, e.g. protein dynamics [21], and energy technologies [22].

The field of multiphysics is very large and we must expect that the hierarchical process of analysis, see references [2, 23], which is in particular applicable to

multiphysics simulations, will be tackled to an increasing extent – in engineering, because new designs require a deeper understanding of performances, and in the sciences, because a deeper understanding of nature through simulations will create important advances – for example, and in particular, in the field of medical sciences.

## **Acknowledgements**

I would like to acknowledge my collaboration with my many students at M.I.T. and colleagues at ADINA R & D, referred to in the references, which has resulted in the research results and developments presented herein.

## **References**

*Due to space limitations, we only refer to some of our publications, however, with numerous references given therein.*

- [1] K.J. Bathe, “The Finite Element Method”, in “Encyclopedia of Computer Science and Engineering”, B. Wah (ed.), J. Wiley and Sons, 1253-1264, 2009.
- [2] K.J. Bathe, “Finite Element Procedures”, Prentice-Hall, 1996.
- [3] D. Chapelle and K.J. Bathe, “The Mathematical Shell Model Underlying General Shell Elements”, Int. J. for Num. Meth. in Eng., 48, 289-313, 2000.
- [4] D. Chapelle and K.J. Bathe, “The Finite Element Analysis of Shells – Fundamentals”, Springer, first edition 2003, second edition 2011.
- [5] D. Chapelle and K.J. Bathe, “On the Ellipticity Condition for Model-Parameter Dependent Mixed Formulations”, Comput. & Struct., 88, 581-587, 2010.
- [6] S. Ham and K.J. Bathe, “A Finite Element Method Enriched for Wave Propagation Problems”, Comput. & Struct., 94-95, 1-12, 2012.
- [7] K.J. Bathe, “Conserving Energy and Momentum in Nonlinear Dynamics: A Simple Implicit Time Integration Scheme”, Comput. & Struct., 85, 437-445, 2007.
- [8] K.J. Bathe and G. Noh, “Insight into an Implicit Time Integration Scheme for Structural Dynamics”, Comput. & Struct., 98-99, 1-6, 2012.
- [9] K.J. Bathe and P.S. Lee, “Measuring the Convergence Behavior of Shell Analysis Schemes”, Comput. & Struct., 89, 285-301, 2011.
- [10] P.S. Lee and K.J. Bathe, “The Quadratic MITC Plate and MITC Shell Elements in Plate Bending”, Advances in Eng. Software, 41, 712-728, 2010.

- [11] K.J. Bathe, F. Brezzi and L. D. Marini, “The MTC9 Shell Element in Plate Bending: Mathematical Analysis of a Simplified Case”, *Comput. Mech.*, 47, 617-626, 2011.
- [12] T. Sussman and K.J. Bathe, “3D-Shell Elements for Structures in Large Strains”, in preparation.
- [13] F.J. Montans and K.J. Bathe, “Computational Issues in Large Strain Elasto-Plasticity: An Algorithm for Mixed Hardening and Plastic Spin”, *Int. J. for Num. Meth. in Eng.*, 63, 159-196, 2005.
- [14] D.N. Kim and K.J. Bathe, “A 4-node 3D-Shell Element to Model Shell Surface Traction and Incompressible Behavior”, *Comput. & Struct.*, 86, 2027-2041, 2008.
- [15] Z. Kazancı and K.J. Bathe, “Crushing and Crashing of Tubes with Implicit Time Integration”, *Int. J. Impact Engineering*, 42, 80-88, 2012.
- [16] D.J. Payen and K.J. Bathe, “A Stress Improvement Procedure”, *Comput. & Struct.*, submitted.
- [17] J. Kim and K.J. Bathe, “The Finite Element Method Enriched by Interpolation Covers”, in preparation.
- [18] K.J. Bathe, H. Zhang, and Y. Yan, “The Solution of Maxwell’s Equations in Multiphysics”, in preparation.
- [19] K.J. Bathe and H. Zhang, “Finite Element Developments for General Fluid Flows with Structural Interactions”, *Int. J. for Num. Meth. in Eng.*, 60, 213-232, 2004.
- [20] K.J. Bathe and H. Zhang, “A Mesh Adaptivity Procedure for CFD and Fluid-Structure Interactions”, *Comput. & Struct.*, 87, 604-617, 2009.
- [21] R.S. Sedeh, M. Bathe, and K.J. Bathe, “The Subspace Iteration Method in Protein Normal Mode Analysis”, *J. Computational Chemistry*, 31, 66-74, 2010.
- [22] C. Deilmann and K.J. Bathe, “A Holistic Method to Design an Optimized Energy Scenario and Quantitatively Evaluate Promising Technologies for Implementation”, *International Journal of Green Energy*, 6, 1-21, 2009.
- [23] M.L. Bucalem and K.J. Bathe, “The Mechanics of Solids and Structures – Hierarchical Modeling and the Finite Element Solution”, Springer, 2011.